

# Admittance Force-Based UAV-Wall Stabilization and Press Exertion for Documentation and Inspection of Historical Buildings

Daniel Smrcka, Tomas Baca, Tiago Nascimento, *Member, IEEE*, and Martin Saska, *Member, IEEE*

**Abstract**—An approach that enables autonomous Unmanned Aerial Vehicles (UAV) with onboard sensor-based force control to interact with the indoor walls of historical buildings is proposed in this paper. The motivation for enabling UAVs to be pressed against walls is twofold: 1) it enables providing strong-side lighting on places where a light source needs to be remotely pressed against the wall for documentation by another drone with a camera and 2) it is a technique for enabling remote placement of infrastructure in difficult-to-access indoor locations, e.g., smart sensors for continuous monitoring of temperature and humidity. We propose therefore an admittance force-based control system that enables a UAV to interact with a wall in a stabilized manner at a pre-defined location. The UAV is coupled with a mechanism that can measure the interacting force, allowing the proposed controller to be in constant contact with the wall based on a measured force, and to regulate the force to the amount required by a given application. The proposed approach has been verified through numerous simulations in Gazebo and experiments with real robots in GNSS-denied environments relying solely on onboard sensors.

**Index Terms**—Unmanned Aerial Vehicles, Wall Interaction, Feedback Control, Admittance Control.

## I. INTRODUCTION

**I**N the course of the last ten years, significant progress has been made in the development of autonomous Unmanned Aerial Vehicles (UAVs) [1]. One of possible applications of small multi-rotor VTOL UAVs is documenting and scanning historical buildings for archiving purposes and for planning renovation work. Historical buildings are usually huge and complicated structures with a large number of locations that were not intended to be visited by people after the construction process had been completed. Nowadays, complete documentation and scanning of large historical - often sacred - monuments, such as churches, cathedrals, castles, and chateaux, requires heavy equipment and massive scaffolding. This in turn has time and financial implications.

\*This work has been supported by the CTU grant no SGS20/174/OHK3/3T/13, and by the project no. DG18P020VV069 in program NAKI II”.

All authors are with the Department of Cybernetics, Czech Technical University in Prague, Prague, Czech Republic., e-mail: (see <http://mrs.felk.cvut.cz/>).

T. Nascimento is also with the Lab of Systems Engineering and Robotics (LASER), Department of Computer Systems, Universidade Federal da Paraíba, Brazil.

Manuscript received April 19, 2005; revised August 26, 2015.



Fig. 1: An example of formations used in the task of cooperating smart lighting in the restricted environment of the interiors of historical buildings.

The use of UAVs presents an alternative solution which, due to its flexibility, reduces the time required for documenting large churches from months to hours [2]. Autonomous UAV systems can be deployed without installing any supporting technology [3]. Hidden or difficult-to-access places can be reached easily with a UAV, and the process can be repeatable thanks to automatic on-board control.

Our project aimed at deploying autonomous UAVs and teams of cooperating UAVs for documenting and scanning historical buildings. We have designed a technology that is mature enough to allow us to fly in the proximity of monuments of enormous historical value, and even in locations beyond the line of sight of the UAV’s safety pilot (see [3] and Fig. 1). During deployment of the technology in various historical objects, we have identified numerous challenges that reach beyond other popular UAV applications, e.g., surveillance, monitoring, precision agriculture, and inspection of industrial structures. End-users of the system - restorers, conservationists, historians and owners of historical objects - require more than just technical pictures for computer vision approaches. Inadequate light conditions in difficult-to-access places have turned out to be the biggest barrier to achieving acceptable results, as the illumination in these locations was not historically designed to support observation from the perspective of flying cameras.



Fig. 2: Pictures taken by a UAV with one onboard camera in the abandoned church in Stará voda. Left: A single UAV carrying both a camera and a light. Right: Strong-side lighting provided by another UAV.

Three main lighting techniques are widely used by restorers and historians nowadays, *Three-Point Lighting (3PL)*, *Reflectance Transformation Imaging (RTI)*, and *Strong-Side Lighting (SSL)* [4]–[6]. UAV systems need to be able to use these techniques to provide complex documentation. We have proposed a way to implement the 3PL and RTI techniques using a formation of cooperating UAVs. In our proposed approach, the leader carries a camera, and followers with onboard light sources fly in positions relative to the leader. This approach has been experimentally tested in historical objects [2], [7] (see Figure 2). However, SSL is much more difficult to implement. SSL requires the positioning of followers with a light source relative to the leader, as in the case of 3PL and RTI, but the light source needs to be pressed against the object being documented. Confirmed attachment (by a force-feedback in our case) of the onboard light to the surface ensures an orthogonal configuration between the camera and the light axes, even for a flat surface such as a wall, where the SSL technique is usually applied to detect damage caused by high levels of humidity.

Much has been written about scanning buildings, but the focus is usually on planning the best sensing locations [8]. In addition, only a few studies have considered the use of autonomous vehicles. Our proposed system is designed for deployment in historical monuments with dimensions varying from small chapels up to large cathedrals. By using multi-rotor UAVs, we introduce the advantages of rapid documentation and the opportunity to access locations that humans cannot reach. However, most works on the use of UAVs have deployed UAVs manually in outdoor locations. In most cases, GNSS is required in order to obtain geo-referenced data. For example, the authors of [9] have presented applications that share a considerable number of common characteristics with indoor documentation of historic structures. Another important task in the documentation of historical buildings is the placement of remote sensors for continuous measurements. Long-term sensory data acquisition of this type efficiently supplements the short-term operation of UAVs with a limited flight time. The use of both *Strong-Side Lighting (SSL)* [4]–[6], a lighting technique widely used by restorers and historians, and remote sensors placement for documenting historical buildings requires the UAV to apply a desired pressure on the wall with controlled force. However, the

dynamics that will enable the UAV to approach close to a wall without colliding with it, and press against it in a stable manner is an open issue [10] that requires a UAV force interaction [11]. Gioioso et al. [12] presented a control design that allows a quadrotor to exert a 3D contact force through a rigid tool. The stability of the system was studied in detail, and the desired 3D force with the position of the tool-tip in the body frame was also considered and tested. However, their approach was not validated with an autonomous multi-rotor UAV, had an external localization system, and the touch sensor was placed on the wall, not on the end-effector, which is not possible in the addressed applications.

There is a variety of manners to control the interaction between a UAV and a physical object such as impedance control [13]–[15], force control [16], [17] and admittance control [18]. Many of these works analyze their approach in simulation environments [13], [14], [16]. In our work, we chose the admittance force control approach to investigate its use in the interaction between a UAV and a wall. The main difference between admittance control and impedance control is that the former controls motion after the force is measured, and the latter controls force after motion or deviation from a set point is measured [19].

An example of admittance force control for physical human-UAV interaction was proposed in [20]. The approach takes the desired coordinates and modifies them according to the external forces, because the original coordinates might be unreachable. However, in their work the feedback sensor data is provided by an outside camera tracking system. By contrast, our approach uses an onboard architecture to estimate the state of the multi-rotor UAV (i.e. LIDAR, the onboard camera, and the laser range finder) to be able to use this system in real-world conditions.

Another approach is the one presented in [18]. The approach estimates external forces acting on the quadcopter from position and attitude information and then input to the admittance controller, which modifies the vehicle reference trajectory accordingly. The reference trajectory is tracked by an underlying position and attitude controller. The characteristics of the over all control scheme are investigated for the near-hover case.

Our proposed approach reaches beyond the work introduced above mainly in its ability to stabilize the UAV automatically, and to apply forces on an object in real GNSS-denied environments, without motion capture systems or any other external infrastructure. The algorithm combines an admittance force control approach that enables a UAV to interact with a wall in a given location with a position controller that we designed for precise movement of multi-UAV systems along desired trajectories [21]. In addition, our novel UAV localization and state estimation system [22], which was designed primarily for exploring underground spaces within the DARPA Subterranean Challenge, is integrated to provide a robust estimate of the relative position of the wall for the approaching UAV. Finally, the main innovative contributions

of this approach are the admittance force control approach, and the UAV system for stable positioning on the walls of historical buildings, with SSL and remote sensor placement as target applications.

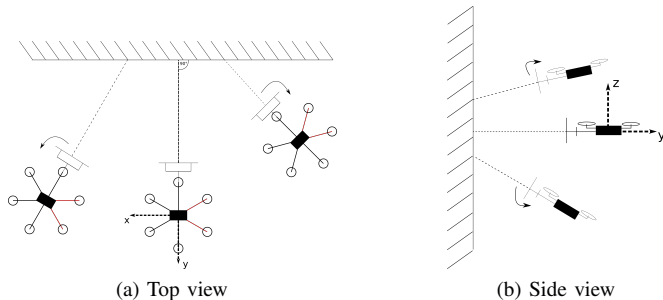


Fig. 3: Possible directions of the approach of the UAV to the wall with the body frame  $[x, y, z]$  of the UAV highlighted.

## II. MECHANISM FOR UAV-WALL INTERACTION WITH SENSORY FEEDBACK

Mechanisms that enable a UAV to interact with a physical object has been the study of recent approaches [23], [24]. In our work, a spring-loaded onboard mechanism with touch sensors was designed to provide robust attachment of the UAV to the wall for the specific applications of SSL and remote placement of micro-scale distance sensors. The mechanism was designed to be as light as possible and to robustly suppress uncertainties in the position and in the tilt of the UAV approaching the wall. Such uncertainties always occur in real applications. During deployment of our autonomous multi-UAV system in historical objects ( $> 20$  historical objects with various features were documented), wind gusts were observed even indoors, at high altitude, mainly close to walls. In addition, dust is always present in places that have not been visited by people for decades or even for centuries. Because of uneven wall surfaces and noisy sensory data due to the dust, the UAV may not approach at the correct angle (Figure 3a), and may not have the ideal tilt (Figure 3b) due to wind compensation close to the wall. The proposed mechanism was therefore designed with two spring-loaded systems to compensate these disturbances. Each of the systems is equipped with sensory feedback to enable admittance force control in real-time.

The sensory feedback used here consists of two button load cells that are accurate force sensors with error within 0.03% to 0.25%. The shape and the dimensions of the contact surface were designed on the basis of numerous tests in manual, semi-autonomous and fully autonomous modes in a church. The following criteria were taken into account: minimal impact on the unstable fragile frescoes, stability during SSL and sensor placement applications, sufficient distance between force sensors to avoid jeopardizing the stabilization when approaching the wall in a wrong direction, where one sensor would be more affected than the other.

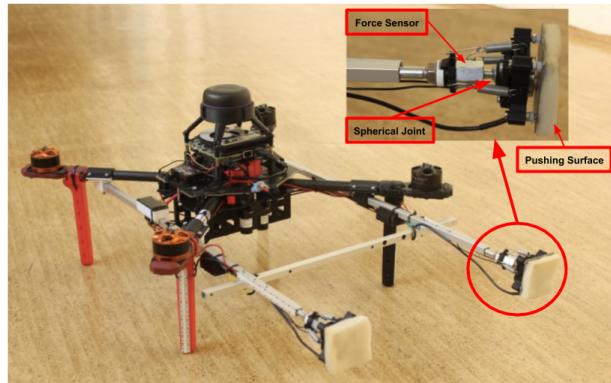


Fig. 4: The Tarot T650 UAV with the wall mechanism designed for autonomous placement of remote sensors.

The final prototype used for experimental verification in this paper is shown in Figure 4 aiming to achieve low weight, high stiffness and fast prototyping.

## III. SYSTEM ARCHITECTURE

The proposed platform consists of several interconnected subsystems. Figure 5 depicts a system diagram of the components within the platform. In the following subsections, we discuss briefly about the State observer, the MPC Wall Tracker and the Feedback controller, focusing on the Admittance Force Controller.

### A. State estimation

The UAV control loop relies on a nonlinear model, which has a translation part:

$$m\ddot{\mathbf{r}} = f\mathbf{R}\hat{\mathbf{e}}_3 - mg\hat{\mathbf{e}}_3 \quad (1)$$

and a rotational part

$$\dot{\mathbf{R}} = \mathbf{R}\boldsymbol{\Omega}, \quad (2)$$

where  $\boldsymbol{\Omega}$  is the tensor of angular velocity, under the condition  $\boldsymbol{\Omega}\mathbf{v} = \boldsymbol{\omega} \times \mathbf{v}, \forall \mathbf{v} \in \mathbb{R}^3$ . A gravitational force with magnitude  $g \in \mathbb{R}$  acts on the vehicle together with the thrust force created collectively by the propellers, and  $m$  stands for the UAV mass.

Estimating the position  $\mathbf{r} = [x, y, z]^T$ , the velocity  $\dot{\mathbf{r}} \in \mathbb{R}^3$ , and the acceleration  $\ddot{\mathbf{r}} \in \mathbb{R}^3$  of the UAV is the focus of this section. The estimation of the rotation matrix from the UAV body frame to the world frame  $\mathbf{R} \in \text{SO}(3) \in \mathbb{R}^{3 \times 3}$  and the angular velocity in the UAV body frame  $\boldsymbol{\omega}$  can be solved individually thanks to the separation of (1) and (2). We consider the estimation of  $\mathbf{R}$  (specifically, the estimation of  $\hat{\mathbf{b}}_3$ ) and  $\boldsymbol{\omega} = [\omega_1, \omega_2, \omega_3]^T$  as provided by an off-the-shelf embedded flight controller<sup>1</sup>. We rely on an attitude control loop, also closed by the embedded flight controller. However, as we are focused on non-aerobatic flight, we separately

<sup>1</sup>We rely on the Pixhawk flight controller for attitude estimation and attitude rate control, <http://pixhawk.com>, <http://px4.io>.

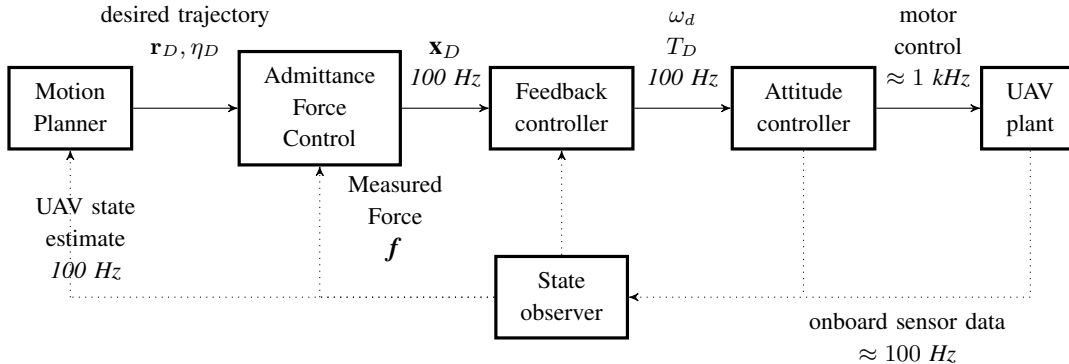


Fig. 5: Control pipeline with admittance control implemented.

consider and estimate the azimuth of the  $\hat{\mathbf{b}}_1$  axis in the world as the UAV *heading*. Under the condition of  $|\hat{\mathbf{e}}_3^T \hat{\mathbf{b}}_1| > 0$ , we define the heading as

$$\eta = \text{atan2} \left( \hat{\mathbf{b}}_1^T \hat{\mathbf{e}}_2, \hat{\mathbf{b}}_1^T \hat{\mathbf{e}}_1 \right). \quad (3)$$

As the 4<sup>th</sup> independently controllable Degree of Freedom DOF, the heading is more intuitive alternative to the commonly used *yaw* angle. It is possible to use it, however, assuming the tilt of the UAV ( $\arccos \hat{\mathbf{b}}_3^T \hat{\mathbf{e}}_3$ ) is low, near horizontal.

The estimation block was proposed on our previous work [21]. In this estimation block, we aimed to apply a simple estimation process by leveraging the specific decoupled structure of the multi-rotor UAV model and utilizing the properties of the proposed controllers. Thus, we model the translation dynamics of the UAV as a point mass in 3-D with an additional degree of freedom in the heading angle,  $\eta$ . The considered state vector for the *high-level* estimation of (1) consists of components of the position  $\mathbf{r}$ , its first two derivatives, and the heading  $\eta$  with its first derivative

$$\mathbf{x} = [x, \dot{x}, \ddot{x}, y, \dot{y}, \ddot{y}, z, \dot{z}, \ddot{z}, \eta, \dot{\eta}]^T. \quad (4)$$

### B. Admittance Force Control (Wall Tracker)

In this section, we propose the admittance force control for the UAV-wall interaction. The final phase of the approach to the wall assumes motion in an environment with no obstacles in the path of the UAV. This is achieved by purpose-designed UAV state estimation techniques [22], by 3D mapping [3], and by high level planning used for documenting historical buildings [7].

Our admittance control takes the desired position coordinates and the measured external forces and gives the coordinates of the reference position coordinates as the output. When the UAV reaches the object (i.e. a wall) and cannot move forward, it controls the position of the UAV to maintain a stable state. Thus, the proposed admittance controller block, shown in Figure 5, takes into account the desired position  $\mathbf{r}_D$ , the desired yaw rotation  $\eta_D$ , and the measured external force  $\mathbf{f}$ . The measured external force is the sum of the

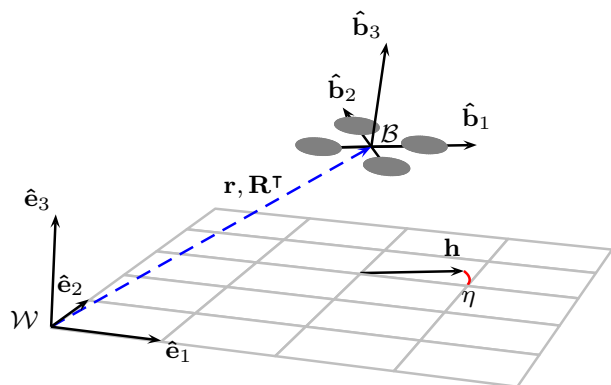


Fig. 6: The world frame  $\mathcal{W} = \{\hat{\mathbf{e}}_1, \hat{\mathbf{e}}_2, \hat{\mathbf{e}}_3\}$ , in which the position and orientation of the UAV body frame  $\mathcal{B} = \{\hat{\mathbf{b}}_1, \hat{\mathbf{b}}_2, \hat{\mathbf{b}}_3\}$  is expressed by translation  $\mathbf{r} = (x, y, z)^T$  and rotation  $\mathbf{R}^T$ , respectively. The UAV heading vector is denoted  $\mathbf{h}$ , and the heading angle is denoted  $\eta$  [21].

forces applied to both force sensors. The control output is the reference position and the yaw angle  $(\mathbf{r}_R, \eta_R)$ . The control output is sent to a wall-tracker, which converts the control output to the position  $\mathbf{r}_D, \dot{\mathbf{r}}_D, \ddot{\mathbf{r}}_D$  and heading commands  $\psi_D, \dot{\psi}_D, \ddot{\psi}_D$ , and sends it to the position controller. The SO(3) controller then produces the orientation and thrust references. The force control therefore begins by estimating the external forces  $\mathbf{f}$  acting on the UAV through the equation

$$M(\ddot{\mathbf{r}}_D - \ddot{\mathbf{r}}_R) + D(\dot{\mathbf{r}}_D - \dot{\mathbf{r}}_R) + K(\mathbf{r}_D - \mathbf{r}_R) = -\mathbf{f}, \quad (5)$$

where  $M, D, K$  are diagonal matrices defining the inertia, the damping and the stiffness of the vehicle, respectively.  $\mathbf{r}_D$  represents the desired coordinates, and  $\mathbf{r}_R$  represents the reference coordinates [20]. This equation reflects the behavior of the UAV when it is pushed.

The representation of the UAV through coordinate systems is presented in Figure 6. The position and orientation of the body frame with respect to the world frame is expressed by the translation vector  $\mathbf{r}$ , and the rotation of the UAV is expressed by rotational matrix  $\mathbf{R}^T$ . We consider the front of

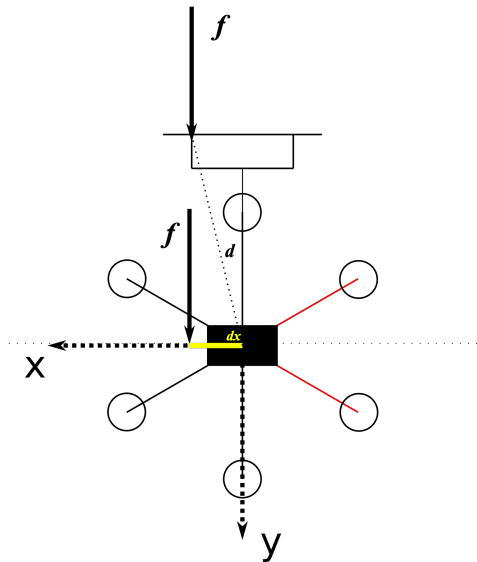


Fig. 7: Example of the force effect on the moment of the UAV.

the UAV as its heading along the x-axis. The mechanism is therefore mounted on the negative side of the y-axis, so we can simplify this equation as follows

$$M(\ddot{r}_{Dy} - \ddot{r}_{Ry}) + D(\dot{r}_{Dy} - \dot{r}_{Ry}) + K(r_{Dy} - r_{Ry}) = -f. \quad (6)$$

Moreover, our force control will consider only the position difference, as it reflects on the applied force. The SO(3) position controller will set the appropriate velocities and accelerations based on the reference position. Thus, we can simplify the equation as follows

$$K(r_{Dy} - r_{Ry}) = -f. \quad (7)$$

Therefore, the controlled reference position  $r_{Ry}$  is expressed as

$$r_{Ry} = r_{Dy} + \frac{f}{K}. \quad (8)$$

However, force control through the position of the UAV is not enough to achieve stabilization. Whenever the UAV approaches the wall from the side, or whenever it applies a force from a different direction, the UAV tries to keep its current yaw angle. We therefore also need to control the yaw angle ( $\eta$ ) of the UAV. To do so, we use the data from both force sensors. The desired yaw angle is calculated through the moment of the force applied to the UAV. Thus, the moment is given as follows

$$\tau = \mathbf{d} \times \mathbf{f}, \quad (9)$$

where  $\mathbf{d}$  is a vector from the center of mass to the point of the applied force  $\mathbf{f}$ .

Now, let us consider the UAV as a solid object. Analyzing Figure 7, we can observe that the force applied to the

mechanism (the corresponding arm  $\mathbf{d}$ ) with respect to the relative movement has the same effect as the equal force applied to the point on the x-axis. This equality can be represented through the following equation

$$\mathbf{d}' \times \mathbf{f}' = \mathbf{d} \times \mathbf{f}. \quad (10)$$

As the force applied to the mechanism has a y-axis value, we can find the corresponding value on the x-axis. This means that the vector is expressed as  $\mathbf{d} = [d_x, 0, 0]'$  and the force vector, which is applied along the y-axis, is  $\mathbf{f} = [0, f_y, 0]'$ . This simplifies the momentum in equation (9) to the multiplication

$$\tau = d_x \cdot f_y. \quad (11)$$

To successfully rotate the UAV into the desired orientation, the goal is to compensate the momentum that is created. Setting the reference yaw to the negated momentum is not ideal, and leads to an unstable state. To correct this problem and to stabilize the UAV, the reference yaw must be the momentum multiplied by a scaling factor  $\alpha = 0.1$ . This scaling factor was empirically estimated throughout the execution of several experiments.

Keeping the UAV stable while touching the wall requires having a particular tilt. As the controlled state in this work is only the position and yaw angle of the UAV, the tilt is controlled indirectly through the reference position. Setting the reference coordinates in the wall (e.g. so that the center of mass of the UAV will try to match the reference coordinate) would result in the UAV exercising a stronger pushing force towards the wall and thus generating the necessary tilt. However, this interaction needs to be controlled on the basis of the measured force to prevent uncontrolled tilt, which would flip the UAV over.

Algorithm 1 summarizes the proposed admittance control system. This algorithm presents two functions. The first function *Get\_Reference* processes the data from the force sensors and calculates the desired movement in the robot body frame ( $\mathcal{C}_x, \mathcal{C}_y, \mathcal{C}_z, \mathcal{C}_\eta$ ). Variable  $f_d$  works as an offset to the applied force. Without the offset, the UAV would be on the threshold between the wall and free flight. Thus, constant contact with the wall would not be assured. The second function *Move\_Relative* performs the transformation of the relative movement into world coordinates. This second function also uses the estimated position and orientation coming from the UAV sensors (*Odom*). The result is added to the desired position. The relative yaw ( $\eta$ ) and the altitude ( $\mathcal{C}_z$ ) of the UAV are directly added to the desired altitude and orientation. During the approaching procedure  $\mathcal{C}_z = 0$ , but for the detaching state  $\mathcal{C}_z = -0.2$ .

The control system is then designed as a state machine consisting of three main states: *approaching*, *stabilization* and *detaching*. The *approaching* state is the default state in the wall-positioning mission. As the name suggests, it is the state that allows the UAV to approach the wall gradually. When

---

**Algorithm 1** The stabilization algorithm that reshapes desired position  $\mathbf{r}_D$  based on external forces.

---

```

1: procedure GET_REFERENCE
2:   Input:
3:      $f_1, f_2$            ▷ data force from the left (1) and right (2) sensors
4:      $\mathbf{r}_D$                ▷ vector of desired position
5:      $f_d$                ▷ desired force set by user
6:   Output:
7:      $\mathbf{r}_R$                ▷ reference position vector
8:      $\eta_R$              ▷ reference yaw orientation
9:      $C_x = 0; C_z = 0;$ 
10:     $f \leftarrow f_1 + f_2$ 
11:     $d_x \leftarrow \frac{\text{sensor\_dist}(2f_1 - f)}{2f}$ 
12:     $C_y \leftarrow \frac{f - f_d}{K_y}$            ▷ desired movement in the body frame
13:     $C_\eta \leftarrow -d_x \cdot f \cdot \alpha$ 
14:     $[\mathbf{r}_R, \eta_R] \leftarrow \text{move\_relative}(C_x, C_y, C_z, C_\eta, \mathbf{r}_D)$ 
15: end procedure

1: procedure MOVE_RELATIVE
2:   Input:
3:      $C_x, C_y, C_z, C_\eta$ 
4:      $\mathbf{r}_D$ 
5:     Odom             ▷ estimated [x, y, z,  $\eta$ ] of the UAV
6:   Output:
7:      $\mathbf{r}_R$ 
8:      $\eta_R$ 
9:      $\mathbf{R} \leftarrow \text{rotationMatrix}(\eta_{\text{Odom}})$ 
10:     $\text{rot} \leftarrow \mathbf{R} \cdot [C_x, C_y]'$            ▷ transformation into world frame
11:     $\mathbf{r}_{Rx} = \text{rot}(1) + r_{Dx}$ 
12:     $\mathbf{r}_{Ry} = \text{rot}(2) + r_{Dy}$ 
13:     $\mathbf{r}_{Rz} = C_z + r_{Dz}$ 
14:     $\eta_R = C_\eta + r_{D\eta}$ 
15: end procedure

```

---

the interaction with the wall occurs, the controller changes to the *stabilization* state. The *stabilization* state runs until the desired position on the wall is changed to another location through an external command from high level planning. When the *detaching* state starts, it sets the reference position further from the wall. To prevent the mechanism from getting stuck on the wall, the UAV sets the reference altitude to minus 20 centimeters,  $C_y = 2$ , and  $C_z = -0.2$  until the UAV detaches from the wall. Then it returns to its original altitude. The admittance force control approach (see Algorithm 1) is used mainly within the *stabilization* and *detaching* states, where there are interaction forces between the UAV and the wall.

After correcting the desired coordinates, the reference pose of the UAV is inserted into the control reference vector  $\mathbf{x}_D$  and sent to the Feedback Controller. The control reference consists of states of the differentially-flat translational dynamics (position, velocity, acceleration, jerk) as well as the heading and the heading rate:

$$\mathbf{x}_D = [x, \dot{x}, \ddot{x}, \overset{\cdot\cdot}{x}, y, \dot{y}, \ddot{y}, \overset{\cdot\cdot}{y}, z, \dot{z}, \ddot{z}, \overset{\cdot\cdot}{z}, \eta, \dot{\eta}]^T. \quad (12)$$

In this work, only the values that came out from Algorithm 1 are filled in the control reference vector  $(\mathbf{r}_R, \eta_R)$ , being the other values zero.

### C. Feedback Control

The feedback controller is a crucial component for controlling flight dynamics around an unstable equilibrium point of the UAV system. The task of a controller is to minimize a control error around the desired control reference  $\mathbf{x}_D$  and to supply feedforward control action according to the states in  $\mathbf{x}_D$ . The control actions produced by a controller within our pipeline are the desired intrinsic angular velocities of the UAV body  $\omega_d \in \mathbb{R}^3$  and the desired collective motor speed  $T_d \in [0, 1]$ .

The feedback control approach we used in our system is a combination of a linear MPC with a nonlinear SO(3) force tracking feedback proposed in our previous work [21]. It was designed to provide a stable feedback even when the UAV state estimate is noisy or unreliable, or when state constraints need to be imposed on the control level.

## IV. RESULTS

As above mentioned, this work forms a part of an ongoing historical building documentation project (NAKI), in which a new UAV platform was designed and built. A second platform, a Tarot T650<sup>2</sup> was used in our experiments and would be used as an automated light holder. This is presented in Figure 4. The results are divided into two parts: simulations and real robot experiments (see the VIDEO<sup>3</sup>). In the video, a final demonstration from a brick wall in an outdoor environment was also performed.

### A. Simulations

Numerous simulations in Gazebo environment were performed with an exact model of the UAV and the force sensor, and in an exact model of a church (see Fig. 8). A desired trajectory is given to the multi-rotor UAV in order to place the UAV in a desired position where the strong-side lighting is ideal (see Fig. 9). A desired force of 5N is therefore exerted in the wall to stable position the UAV as a light source. During the simulations, the UAV responded accordingly and was successful on exerting the desired force into the wall while maintaining a fixed position. The force plot during the period that the pressure was exerted can be seen in Fig. 10. Despite the variation on the input force, the robot was able to exert the desired pressure in a stable manner.

### B. Real Robot Experiments

The experiment with a real robot aimed to demonstrate the effectiveness of the approach when the UAV is set to touch the wall, applying the force during 10s. In many cases, the wall of a historical building is fragile and only a limited amount of force can be exerted on the wall. Therefore, a trajectory is needed that enables the multi-rotor UAV only

<sup>2</sup>For a better hardware detail on the UAV platform, please visit <http://mrs.felk.cvut.cz/research/micro-aerial-vehicles>

<sup>3</sup><http://mrs.felk.cvut.cz/admittance-force-control>



Fig. 8: Simulation environment.



(a) Top view.



(b) Side view.

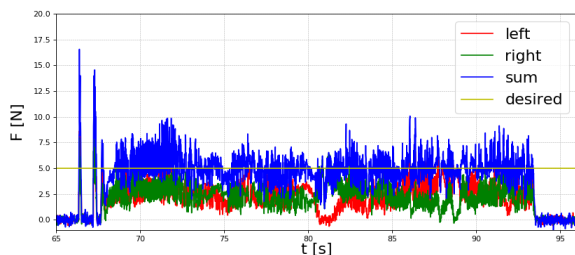
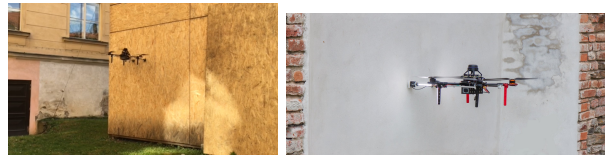
Fig. 9: Simulation experiment<sup>3</sup>.

Fig. 10: Detailed section of the force plot from the church simulation.

gently to touch the wall and flash the strong-side light. In the experiment, it was verified that the proposed architecture is able to control the robot to touch the wall with minimum impact. Figure 11 details the performed experiment.

Furthermore, we can note on Fig. 13a that in an initial moment the reference trajectory and odometry is used to



(a) Wooden wall.

(b) Brick wall.



(c) Stone wall.

Fig. 11: Experimental environment.

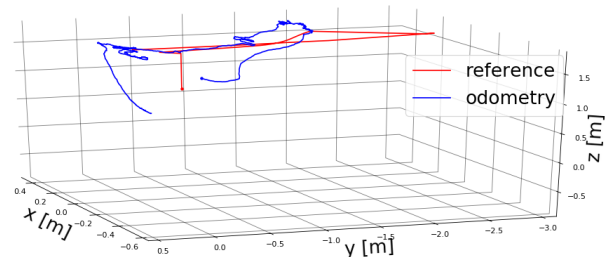
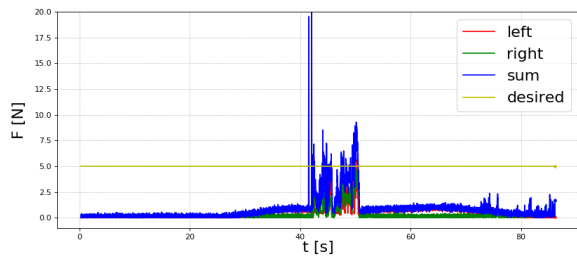


Fig. 12: Robot trajectory plot.

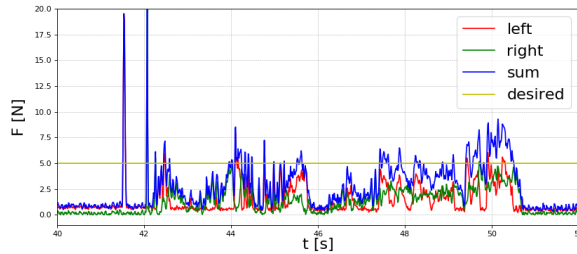
bring the multi-rotor UAV near to the wall within the first 40 s. The wall is detected and the drone is localized using onboard sensors and computational power (RP-Lidar acts as the core sensor). The data record indicates that the applied force was  $\approx 5N$  and the experiment verified appropriate execution of the desired task, as Fig. 13b demonstrates in detail. The noisy behavior observed on the plots are due to the measurement on the force sensors. This can be mitigated with a force estimator. Nevertheless, we can observe that despite the noise, the controller behaves properly. Finally, the UAV performs a trajectory that enables a careful approximation to the wall (see Fig. 12). This enables the UAV to avoid damaging the wall frescoes or a collision within another part of a wall in a indoor environment.

## V. CONCLUSION

This work has presented a solution to the problem of the controlled interaction of an Unmanned Aerial Vehicle with interior walls of large buildings using a compliant mechanism. We have proposed an admittance control technique based on the measured force of two force sensors while attached to the wall. A spring-loaded mechanism with two



(a) Whole experiment.



(b) Detailed section.

Fig. 13: Force plot from the experiment<sup>3</sup>.

sensory systems providing feedback in real time was mounted on the y-axis of the UAV, providing a reliable response while attached to the wall. Using this approach, the UAV proved to be capable of exerting a given force for a given time interval, which is required by both target applications - the strong-side light technique and remote sensors attachment in historical buildings.

## REFERENCES

- [1] T. P. Nascimento and M. Saska, "Position and attitude control of multi-rotor aerial vehicles: A survey," *Annual Reviews in Control*, vol. 48, pp. 1367–5788, 2019.
- [2] M. Saska, V. Krátky, V. Spurny, and T. Baca, "Documentation of dark areas of large historical buildings by a formation of unmanned aerial vehicles using model predictive control," in *IEEE ETFA*, 2017.
- [3] P. Petráček, V. Krátký, and M. Saska, "Dronument: System for Reliable Deployment of Micro Aerial Vehicles in Dark Areas of Large Historical Monuments," in *IEEE Robotics and Automation Letters (In Press: Accepted for publication on January 7, 2020)*, 2020.
- [4] Y. Zhang and K.-L. Ma, "Lighting design for globally illuminated volume rendering," *IEEE Transactions on Visualization and Computer Graphics*, vol. 19, pp. 2946–2955, 2013.
- [5] D. Saunders, R. Collmann, and A. Borda, "Reflectance transformation imaging and imagej: Comparing imaging methodologies for cultural heritage artefacts," in *EVA*, 2017.
- [6] Y. H. Kim, J. Choi, Y. Y. Lee, B. Ahmed, and K. H. Lee, "Reflectance transformation imaging method for large-scale objects," in *CGiV*, 2016.
- [7] V. Krátký, P. Petráček, V. Spurný, and M. Saska, "Autonomous Reflectance Transformation Imaging by Team of Unmanned Aerial Vehicles," in *IEEE Robotics and Automation Letters (In Press: Accepted for publication on January 15, 2020)*, 2020.
- [8] D. Cowley *et al.*, "UAVs in Context: Archaeological Airborne Recording in a National Body of Survey and Record," *Drones*, vol. 2, p. 2, 2017.
- [9] M. Beul *et al.*, "Fast Autonomous Flight in Warehouses for Inventory Applications," *IEEE RA-L*, vol. 3, no. 4, pp. 3121–3128, 2018.
- [10] F. Chui, G. Dicker, and I. Sharf, "Dynamics of a quadrotor undergoing impact with a wall," in *2016 International Conference on Unmanned Aircraft Systems (ICUAS)*, June 2016, pp. 717–726.
- [11] G. Dicker, F. Chui, and I. Sharf, "Quadrotor collision characterization and recovery control," in *2017 IEEE International Conference on Robotics and Automation (ICRA)*, May 2017, pp. 5830–5836.
- [12] G. Gioioso, M. Ryll, D. Prattichizzo, H. H. Bühlhoff, and A. Franchi, "Turning a near-hovering controlled quadrotor into a 3d force effector," in *2014 IEEE International Conference on Robotics and Automation (ICRA)*, May 2014, pp. 6278–6284.
- [13] V. Lippiello and F. Ruggiero, "Exploiting redundancy in cartesian impedance control of uavs equipped with a robotic arm," in *2012 IEEE/RSJ International Conference on Intelligent Robots and Systems*, 2012, pp. 3768–3773.
- [14] F. Forte, R. Naldi, A. Macchelli, and L. Marconi, "Impedance control of an aerial manipulator," in *2012 American Control Conference (ACC)*, 2012, pp. 3839–3844.
- [15] A. Suarez, G. Heredia, and A. Ollero, "Physical-virtual impedance control in ultralightweight and compliant dual-arm aerial manipulators," *IEEE Robotics and Automation Letters*, vol. 3, no. 3, pp. 2553–2560, 2018.
- [16] S. Bellens, J. De Schutter, and H. Bruyninckx, "A hybrid pose / wrench control framework for quadrotor helicopters," in *2012 IEEE International Conference on Robotics and Automation*, 2012, pp. 2269–2274.
- [17] H. W. Wopereis, J. J. Hoekstra, T. H. Post, G. A. Folkertsma, S. Stramigioli, and M. Fumagalli, "Application of substantial and sustained force to vertical surfaces using a quadrotor," in *2017 IEEE International Conference on Robotics and Automation (ICRA)*, 2017, pp. 2704–2709.
- [18] F. Augugliaro and R. D'Andrea, "Admittance control for physical human-quadrocopter interaction," in *2013 European Control Conference (ECC)*, 2013, pp. 1805–1810.
- [19] A. Q. Keemink, H. van der Kooij, and A. H. Stienen, "Admittance control for physical human-robot interaction," *The International Journal of Robotics Research*, vol. 37, no. 11, pp. 1421–1444, 2018.
- [20] F. Augugliaro and R. D'Andrea, "Admittance control for physical human-quadrocopter interaction," in *2013 European Control Conference (ECC)*, July 2013, pp. 1805–1810.
- [21] T. Baca, M. Petrlik, M. Vrba, V. Spurny, R. Penicka, D. Hert, and M. Saska, "The MRS UAV System: Pushing the Frontiers of Reproducible Research, Real-world Deployment, and Education with Autonomous Unmanned Aerial Vehicles," *Journal of Intelligent & Robotic Systems*, vol. 102, no. 26, pp. 1–28, May 2021.
- [22] M. Petrlik, T. Báča, D. Heřt, M. Vrba, T. Krajník, and M. Saska, "A robust uav system for operations in a constrained environment," *IEEE Robotics and Automation Letters (RAL)*, 2020.
- [23] T. Bartelds, A. Capra, S. Hamaza, S. Stramigioli, and M. Fumagalli, "Compliant aerial manipulators: Toward a new generation of aerial robotic workers," *IEEE Robotics and Automation Letters*, vol. 1, no. 1, pp. 477–483, 2016.
- [24] T. Ikeda, S. Yasui, M. Fujihara, K. Ohara, S. Ashizawa, A. Ichikawa, A. Okino, T. Oomichi, and T. Fukuda, "Wall contact by octo-rotor uav with one dof manipulator for bridge inspection," in *2017 IEEE/RSJ International Conference on Intelligent Robots and Systems (IROS)*, Sep. 2017, pp. 5122–5127.